Selective excitation of the OClO molecule with femtosecond laser pulse

Kai-Jun Yuan
Department of Physics, Dalian University of Technology, Dalian 116024, People's Republic of China

Zhigang Sun
State Key Laboratory of Molecular Reaction Dynamics, Dalian Institute of Chemical Physics, Chinese Academy of Sciences, Dalian 116023, People's Republic of China

Shu-Lin Cong*
Department of Physics, Dalian University of Technology, Dalian 116024, People's Republic of China

Nanquan Lou
State Key Laboratory of Molecular Reaction Dynamics, Dalian Institute of Chemical Physics, Chinese Academy of Sciences, Dalian 116023, People's Republic of China

(Received 30 August 2005; published 23 November 2005)

The three-dimensional time-dependent quantum wave packet dynamics ($J=0$) using a Hamiltonian for a triatomic molecule in Radau coordinates is employed to study laser pulse excitation of the OClO molecule. The fast Fourier transform (FFT) and the split operator methods are applied to propagate the wave packet. The vibronic excitations $A\,^2A_2(\nu_1,\nu_2,\nu_3)\leftarrow X\,^2B_1(0,0,0)$ of the triatomic molecule OClO using femtosecond laser pulses of varying intensities are investigated. With an ultrashort laser pulse of certain FWHM (full width at half maximum), the vibrational level can be selectively excited. The changes in the vibrational population distributions caused by simple variation of the pulse are remarkable.

DOI: 10.1103/PhysRevA.72.052513 PACS number(s): 33.20.Tp, 33.70.−w, 33.90.+h

I. INTRODUCTION

Control of molecular dynamics by laser pulse is one of the major and ultimate goals of photophysics and photochemistry [1]. The relevant laser parameters, such as the intensity, the width, and the shape of the pulse, have been used to control the molecular excitation. The technique of ultrashort intense laser pulses has led to the observation of many interesting strong field phenomena in atoms and molecules including bond softening and hardening [2], above threshold ionization and dissociation [3,4], intact ionization of large polyatomic molecules [5], transient field-induced resonance [6], and adiabatic passage of light-induced potentials [7]. Most of these phenomena can be quantitatively understood using the concept of light-dressed potential energy surfaces [8–11].

The potential of steering the molecular dynamics with optimally shaped femtosecond laser pulses has been pointed out as a coming frontier. Femtosecond real-time pump-probe experiments together with *ab initio* quantum calculations and simulations have been used to interpret the optimal control of the $CpMn(CO)_5$ and $CpMn(CO)_3$ molecules [12,13]. The influence of the chirp and the separation of subpulses in pulse trains, which are simple control parameters in the optimal pulses, have been experimentally investigated for NaK and Na_2K molecules [14].

It is known that vibrational preexcitation may affect several intermolecular properties [15,16]. Owing to the participation of more than one excited potential energy surface (PES), different access of the upper PESs might lead to adiabatic or nonadiabatic processes resulting in different photodissociation pathways and influence the branching ratio between different fragments. In the excitation dynamics of the $A\,^2A_2$ state of the OClO molecule, mode specific $Cl+O_2$:$ClO+O$ branching ratios from different initial vibrational levels has been observed [17]. Relative to pure symmetric stretching modes $(\nu_1,0,0)$, the Cl yield is slightly enhanced for combination bands containing one quantum of bending $(\nu_1,1,0)$ and significantly diminished for neighboring $(\nu_1-1,0,2)$ levels having asymmetric stretching excitation.

In this paper, we will show that it is possible to selectively excite vibrational levels even with a laser pulse of broad spectral range by using stimulated emission pumping (Rabi floppings) in competition with nuclear dynamics of the multi-mode vibrational motions of the OClO molecule. With the full dimensionality quantum wave packet dynamics calculations based on the Born-Oppenheimer approximation, the interaction processes of the OClO molecule between the ground $X\,^2B_1$ and the excited $A\,^2A_2$ states via ultrashort transform-limited laser fields of varying intensities are studied. It is found that we can excite a special vibrational mode among neighboring levels by trivially changing the intensity of a specified ultrashort femtosecond laser pulse with proper width. The underlying physical mechanism has close relation to ac-Stark shift and Rabi oscillations within the duration of the laser pulse and to the influence of the nuclear motion on the excited states.

The OClO molecule is of both experimental and theoretical interest, for instance for its role in polar stratospheric

*Author to whom correspondence should be addressed. Electronic address: shlcong@dlut.edu.cn

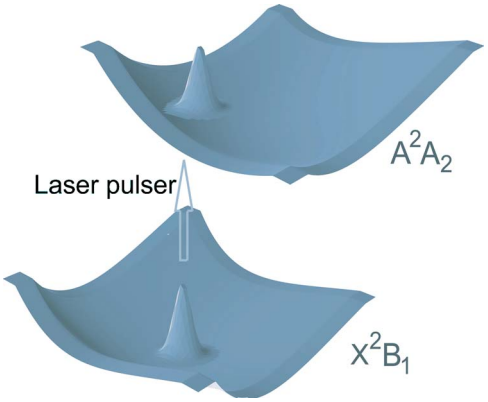

FIG. 1. (Color online) Schematic illustration of the potential energy surfaces used in our study of the OClO molecule and the laser excitation process.

ozone depletion [18]. Accurate PESs of the ground $X\,^2B_1$ and the first excited $A\,^2A_2$ state are available [19,20]. Transitions between these states give rise to photon absorption of visible light. The *ab initio* PES of the state $X\,^2B_1$ includes nonharmonic (higher order) coupling between the asymmetric stretch, the symmetric stretch, and bend vibrations. This PES may reproduce the experimentally observed asymmetric vibrational peaks in the photoabsorption spectrum. These peaks would be forbidden assuming C_{2v} symmetry for both the $X\,^2B_1$ and $A\,^2A_2$ states and only a harmonic oscillator function, which also is experimentally interpreted as the result of a double minimum in the asymmetric stretch potential function [21]. The OClO molecule has been studied by several groups using ultrashort laser pulses [22–24]. This motivates us to further study laser pulse excitation dynamics using the triatomic OClO molecule as prototype.

The paper is arranged as follows: In Sec. II we briefly present the computational details of three-dimensional time-dependent wave packet calculations. The vibrational excitations of the OClO molecule in the femtosecond pulse laser field are discussed in Sec. III. We summarize our findings in Sec. IV.

II. COMPUTATIONAL ASPECTS

Our numerical simulations include the two electronic states, $X\,^2B_1$ and $A\,^2A_2$, of OClO and a transform-limited ultrashort femtosecond pulse. The *ab initio* PESs of the ground $X\,^2B_1$ and excited $A\,^2A_2$ states given by Peterson [19], which can be better reproduced in the absorption spectrum [25], are used. The laser excitation and the PESs are depicted in Fig. 1. In this figure, the Cl-O bonds, r_1 and r_2, are varied while the angle between them is fixed at the equilibrium value.

For a light-heavy-light molecule, such as OClO, Radau coordinates (R_1,R_2,φ) are a usual choice [26,27]. The two radial stretching coordinates, R_1 and R_2, measure the distance of the two end light atoms from the canonical point and the third coordinate φ represents the angle between R_1 and R_2. For OClO, the used Hamiltonian can be written as

TABLE I. The spatial grid parameters R_1, R_2, and φ of OClO.

	Min	Max	Grid points
$R_1(a_0)$	2.1	3.8	64
$R_2(a_0)$	2.1	3.8	64
φ(rad)	1.9	2.95	32

$$\hat{H} = -\frac{\hbar^2}{2m_O}\frac{\partial^2}{\partial R_1^2} - \frac{\hbar^2}{2m_O}\frac{\partial^2}{\partial R_2^2} - \frac{\hbar^2}{2m_O}\left(\frac{1}{R_1^2}+\frac{1}{R_2^2}\right)\frac{\partial^2}{\partial \varphi^2} + \Delta\hat{V} + \hat{V}(R_1,R_2,\varphi), \tag{1}$$

with

$$\Delta\hat{V} = -\frac{\hbar^2}{2m_O}\left(\frac{1}{R_1^2}+\frac{1}{R_2^2}\right)\left(\frac{1}{4\sin^2\varphi}+\frac{1}{4}\right). \tag{2}$$

The volume element for $\hat{H}$ in Eq. (1) is $\alpha^{-3}dR_1dR_2d\varphi$, where $\alpha^2 = m_{Cl}/(2m_O+m_{Cl})$.

The PESs of the $X\,^2B_1$ and $A\,^2A_2$ states are coupled by a femtosecond laser field, whereby the time-dependence wave function of the OClO molecule is given by

$$\begin{pmatrix}\Psi_A(t)\\ \Psi_X(t)\end{pmatrix} = \exp\left[-i\int_0^{t_0}\begin{pmatrix}H_A & \mu E(t')\\ \mu E(t') & H_X\end{pmatrix}dt'\right]\begin{pmatrix}0\\ \Phi_0\end{pmatrix}, \tag{3}$$

where μ is the transition dipole moment between the ground and excited states which has not been calculated yet. An arbitrary value of 4.0 a.u. is used and the Condon approximation is invoked. Φ_0 is the initial wave packet on the ground state which is found by a three-dimensional Fourier grid Hamiltonian method [26]. The molecular wave packet is propagated in Radau coordinates on a Fourier grid using the split operator method combined with the fast Fourier transform (FFT) technique [26–28]. The laser field $E(t)$ is given by

$$E(t) = E_0F(t)\cos(\omega t) \tag{4}$$

with

$$F(t) = \exp\left[-4\ln 2\left(\frac{t}{T}\right)^2\right]. \tag{5}$$

Here ω decides the photon energy of the laser pulse and E_0 is the amplitude of the laser field. $F(t)$ denotes the Gaussian pulse envelope with a FWHM (full width at half maximum) T.

The parameters used in the calculations are listed in Table I. In order to propagate the vibrational wave packet on the grid by using the split operator method on the coupled PESs, usually the potential matrix of the Hamiltonian is diagonalized. Here we apply a procedure which reduces to a simple matrix multiplication that is numerically most appealing [29]. The time step in this study is always set to 0.1 fs which is sufficient to obtain converged results.

The vibrational distribution of the excited state is determined by the Fourier transform $F(\omega)$ of the autocorrelation function $C(t)$ of the excited state wave packet [30]. $C(t)$ and $F(\omega)$ can be expressed as

$$C(t) = \langle \Psi_A(t_0) | \Psi_A(t - t_0) \rangle \tag{6}$$

and

$$F(\omega) = 2\,\mathrm{Re}\left(\int_{t_0}^{T_t} C(t) e^{iE(t-t_0)} dt \right). \tag{7}$$

$\Psi_A(t_0)$ is the excited state wave packet just after the laser pulse has passed [31]. Before the time autocorrelation function is Fourier transformed to obtain the population distribution, it is first damped with an exponential function $f(t)$,

$$C'(t) = C(t) f(t) = C(t) \exp(-t/\tau). \tag{8}$$

This results in broadened spectral peaks as the autocorrelation function vanishes after a shorter propagation. The parameter τ in Eq. (8) is chosen to obtain a good peak-to-peak resolution. In the absorption spectrum calculation, this corresponds to convoluting the spectrum with a Lorentzian function of FWHM $\Gamma = 2/\tau$. When the initial wave function is the eigenfunction of the ground vibrational level of the $X\,^2B_1$ state, we can obtain the corresponding Franck-Condon factors between the two electronic states [30].

We only perform the calculations for $J=0$. The zero angular momentum approximation is believed to be credible for this ultra-fast excitation process [32]. We also neglect the multiphoton excitation and vibronic coupling to other electronic states, as they are believed to be of minor importance to the issues of interest here [33,34]. One of the drawbacks of the numerical model is the negligence of the high-lying electronic states and the nearby $^2A_2$ and $^2B_1$ states. Therefore, the accompanying transition from ground state to the electronic states other than the $A\,^2A_2$ state, which may take place in reality, are not taken into account in our calculations. However, the lowest high-lying state above the $A\,^2A_2$ state has the vertical excitation energy of 6.82 eV [35] which implies that it is difficult for multiphoton transition to happen considering the used photon energy in the calculation. Further, the nearby $^2A_1$ state is of vanishing absorption and the state $^2B_2$ is optically dark, whose influence on the coupling between the $A\,^2A_2$ and $^2B_2$ states via the femtosecond laser pulse is negligible, even with a strong laser field [36]. As a result, the present model may be regarded as an effective simplification.

III. RESULTS AND DISCUSSIONS

We first present the absorption spectrum, in Fig. 2, for the $A\,^2A_2 \leftarrow X\,^2B_1$ transition before we discuss the laser excitation of the OClO molecule. The damping function Γ is chosen as 4.5×10^{-5} a.u. The product of spectral components decides the vibrational population distributions after a laser pulse excitation. The reference level of the energy coordinate of Fig. 2 is the vibrational minimum of the PES of the $X\,^2B_1$ state. The zero point energy of the ground vibrational state of the $X\,^2B_1$ state is 1264 cm^{-1}. Comparing the calculated results in Fig. 2 with the experimental absorption spectrum [21], a good agreement is found, which motivates the use of the *ab initio* PESs [19] in this work.

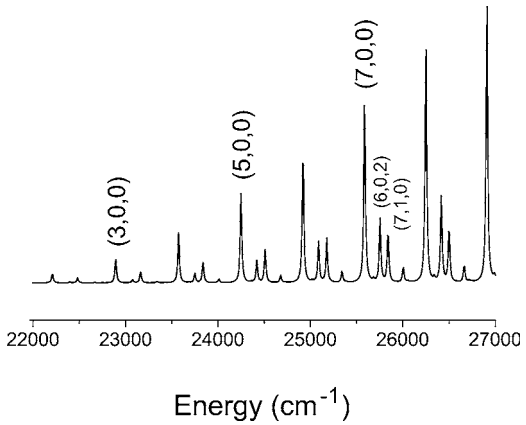

FIG. 2. The partial absorption spectrum of the $O^{35}ClO$ molecule for the $A\,^2A_2 \leftarrow X\,^2B_1$ transition. The zero of energy is the ground vibrational level of the $X\,^2B_1$ state.

In the following, we will show that by varying the peak intensity with proper FWHM, a femtosecond laser pulse can selectively excite vibrational levels of OClO molecules. Our work here is just an exploratory study to show that it is possible to make use of the competition between stimulated emission and nuclear motion to selectively excite a molecule with an femtosecond laser pulse. The objective is to control the relative population on the vibrational level (7,0,0), (6,0,2), and (7,1,0) of the triatomic molecule OClO. In the excitation processes, the spectral distributions decide the population distributions of the vibrational levels.

From Fig. 2, we can see that the energy of the vibrational level (7,0,0) is 25 814 cm^{-1} and that of (6,0,2) is 25 985 cm^{-1} on the PES of the $A\,^2A_2$ state. Therefore we choose the central wavelength of the laser pulse as 25 866 cm^{-1} (386.6 nm) which is between the two levels. Here we have shifted T_e upwards by 230 cm^{-1}, compared to the reported *ab initio* value [25]. This makes the positions of the involved levels of the PES of the $A\,^2A_2$ state better agree with those of the experimental values.

In Fig. 3, we show the dynamics of the excited $A\,^2A_2$ state of the OClO molecule induced by the laser pulses centered at 386.6 nm with the FWHM of 20 fs which is shorter than the vibrational period of the (7,0,0), (6,0,2), and (7,1,0) modes. The vibrational population distributions shown in the left panels reflect the corresponding Franck-Condon factors involving the ground vibrational level of the $X\,^2B_1$ state. In the right panels no obvious Rabi oscillation appears even though with intense laser pulses. This is because the population on the $A\,^2A_2$ excited by the leading part of the laser pulse has moved away from the interaction region before Rabi oscillation occurs. From the left panels, we can see that more vibrational levels are excited with the stronger laser pulse than the weaker pulse. Increasing the intensity, the excited levels have been shifted down towards lower energy. This is caused by the large ac-Stark shift. Furthermore, we can also see that, with the intensity of 1.0×10^{12} $\mathrm{W/cm}^2$, the bending and asymmetric stretch modes, (6,0,2) and (7,0,1), acquire rela-

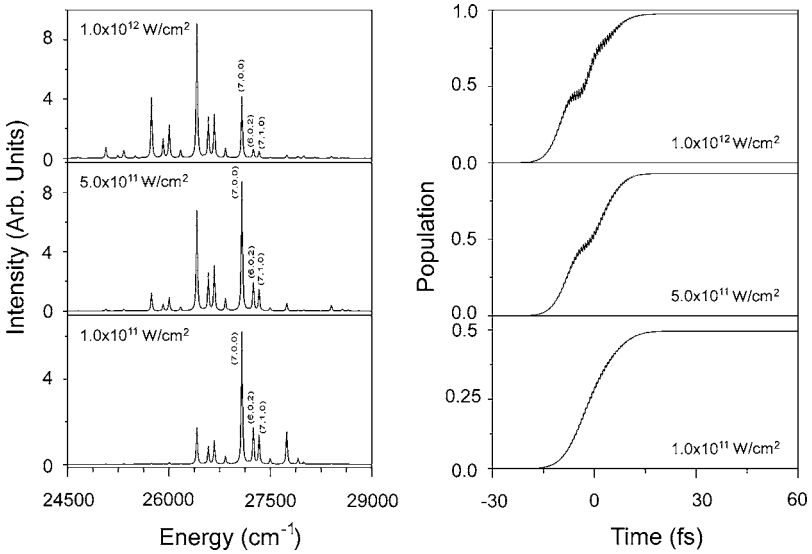

FIG. 3. Left panels: The population distributions on vibrational levels of the $A\,^2A_2$ state for the 20 fs pulse excitation with varying intensities. Right panels: the corresponding time-dependent population of the excited $A\,^2A_2$ state. The zero of energy is taken as the minimum of the potential energy surface of the $X\,^2B_1$ state.

tively less population after the stronger excitation. This results from the slow motion of the bending and asymmetric stretch which makes Rabi oscillation more effective for these states.

In Fig. 4 we display the vibrational distributions and the corresponding time-dependent population of the excited $A\,^2A_2$ state with laser pulses of different intensities. The FWHM of the laser pulse has been chosen to be 80 fs, which is longer than the vibrational period of the symmetric stretch (7,0,0) but shorter than those of bend (7,1,0) and asymmetric stretch (6,0,2) modes. It can be seen that we may control the population of the vibrational levels (7,0,0), (6,0,2), and (7,1,0). With the increase of the laser intensity, the ratio of the population of the three vibrational states changes. With

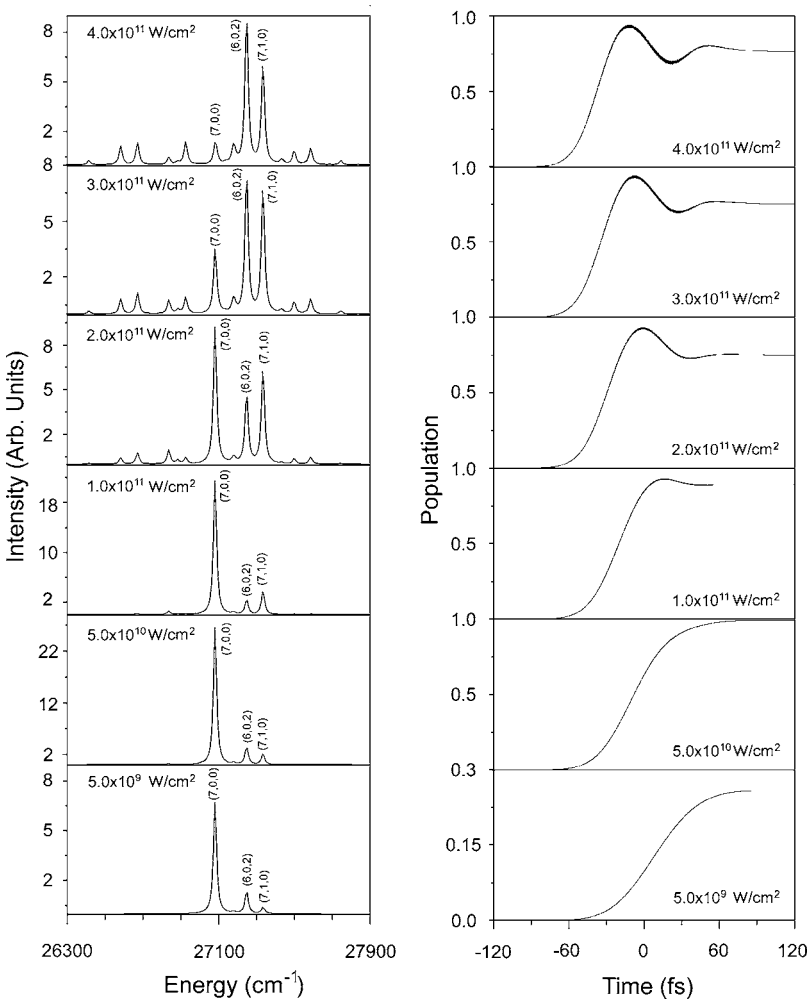

FIG. 4. Left panels: The population distributions on vibrational levels of the $A\,^2A_2$ state for the 80 fs pulse excitation with varying intensities. Right panels: the corresponding time-dependent population of the excited $A\,^2A_2$ state. The population ratio of the vibrational levels (7,0,0), (6,0,2), and (7,1,0) are progressively changed, demonstrated by the variation of the corresponding peaks in the left panels. The zero of energy is taken as the minimum of the potential energy surface of the $X\,^2B_1$ state.

the intensity of 5×10^9 W cm^{-2}, the population of the excited state is dominantly excited to the vibrational level (7,0,0). Increasing laser intensity, the excited population of (7,0,0) relatively decreases. When the intensity is 4×10^{11} W cm^{-2}, the peak of (7,0,0) become vanishing but those of (6,0,2) and (7,1,0) turn into being dominant. In other words, by varying the peak intensity of the laser pulses, we can selectively excite vibrational levels with high efficiency.

The symmetric stretch, asymmetric stretch, and bend vibrational modes of the OClO molecule can be regarded as three one-dimensional models. For the excited $A\,^2A_2$ state, the vibrational periods of the symmetric stretch (7,0,0), asymmetric stretch (6,0,2), and bend (7,1,0) modes are 47, 83, and 116 fs, respectively [22]. In the case of a very intense laser field, where the bare potential energy surfaces have been drastically distorted, the explanation based upon one-dimensional models may not work. However, for laser pulses of up to 4.0×10^{11} W/cm^2, the explanation should be reasonable.

The excited population $P(t)$ follows the area-theorem as $P(t)\propto\sin^2\sigma(t)$, where $\sigma(t)=\int_{-\infty}^{t}E_0F(t')dt'$ is pulse area [37]. For the weak laser pulse, the final population residing on the excited potential only depends on the pulse area and the Franck-Condon factor. With increasing the intensity of the excited pulse, the Rabi oscillation appears in the time-dependent population when the pulse area is larger than 2π, as shown in the right panels of Fig. 4. Moreover, the FWHM of the laser pulse is 80 fs, which is far from a δ-function pulse for the three one-dimensional modes. Therefore, during the intense interaction the dynamics of the excited wave packet plays a prominent role [37,38]. The vibrational period of the excited state of the symmetric stretch mode is much shorter than those of the asymmetric stretch and bend modes, therefore the initial wave packet excited to the upper curve of the symmetric mode moves away faster than those of the asymmetric stretch and bend modes. For each one-dimensional mode with the intense excitation, the leading edge of the pulse progressively transfers the population from ground state to the excited state. Simultaneously the wave packet moves away from resonance region of the excited state and the excitation is complete after the first half of a Rabi oscillation. When being excited by the tailing edge of the laser pulse, the excited wave packet of the symmetric stretch mode returns to the resonance region again and the population of the excited state is completely transferred to the ground state. For asymmetric stretch and bend modes, on the other hand, which have a longer vibrational period, the wave packet does not have enough time to return to the resonance region before the end of the laser pulse. Therefore most of the population of the excited state transferred by the leading edge of the pulse still remains on the excited state even though it has experienced a laser excitation of the same pulse area. As a result, the final excitation efficiencies by the identical laser pulses are quite different for these three modes.

We note here the ratio between the (6,0,2) and (7,1,0) peaks progressively changes with increasing laser intensity as shown in Fig. 4. This may reflect the different anharmonic couplings between the symmetric stretch and the bend modes and between the symmetric and asymmetric stretch modes. The initial decrease in the (7,0,0) level pulls down some population on the (6,0,2) level because of their strong coupling. We also see that the relative population of the (7,0,0) peak excited by the pulse peak intensity of 5×10^{10} W cm^{-2} is relatively more than that for 5×10^9 W cm^{-2}, which is contrary to the discussion above. This results from the increased ac-Stark shift with increasing laser intensity which plays a dominant role before the Rabi oscillation appears.

Based upon the above discussion, it is clear that it is possible to selectively excite vibrational levels with certain laser pulses by varying their peak intensities. The choice of the laser pulse is quite important and it can be optimized further. With a proper laser pulse, we can even expect selective excitation between neighboring peaks of the asymmetric stretch and bend modes is effective.

IV. CONCLUSION

We have studied theoretically the vibrational excitation of the OClO molecule in the laser fields with different intensities and widths of pulses. Choosing proper FWHM and intensity of the pulse can substantially change the excitation of different vibrational levels. We have demonstrated that it is possible to control the excitation of special vibrational levels of the excited state of the OClO molecule by varying the peak intensity and width of laser pulse. The femtosecond ultrashort laser pulses should be powerful for controlling the excitation of a triatomic molecule when a shaped laser pulse is used. We believe that the results presented here may be helpful to qualitatively understand the experimental results.

ACKNOWLEDGMENT

This work was supported by the National Science Foundation of China under Grant No. 10374012.

[1] A. D. Bandrauk, *Molecules in Laser Fields* (Marcel Dekker Inc., New York, 1994).
[2] A. Giusti-Suzor and F. H. Mies, Phys. Rev. Lett. **68**, 3869 (1992).
[3] P. Agostini, F. Fabre, G. Mainfray, G. Petite, and N. K. Rahman, Phys. Rev. Lett. **42**, 1127 (1979).
[4] A. Zavriyev, P. H. Bucksbaum, J. Squier, and F. Saline, Phys. Rev. Lett. **70**, 1077 (1993).
[5] M. J. Dewitt and R. J. Levis, J. Chem. Phys. **102**, 8670 (1995).
[6] R. R. Freeman and P. H. Bucksbaum, J. Phys. B **24**, 325 (1991).
[7] B. M. Garraway and K. A. Suominen, Phys. Rev. Lett. **80**, 932 (1998).
[8] A. Giusti-Suzor, F. H. Mies, L. F. Dimauro, E. Charron, and B.

Yang, J. Phys. B **28**, 309 (1995).
[9] H. Umeda and Y. Fujimura, J. Chem. Phys. **113**, 3510 (2000).
[10] I. R. Solá, B. Y. Chang, J. Santamaría, V. S. Malinovsky, and J. L. Krause, Phys. Rev. Lett. **85**, 4241 (2000).
[11] K. J. Yuan, Z. G. Sun, S. L. Cong, S. M. Wang, J. Yu, and N. Q. Lou, Chem. Phys. **316**, 245 (2005).
[12] C. Daniel, J. Full, L. Gonzáles, C. Lupulescu, J. Manz, A. Merli, Š. Vajda, and L. Wöste, Science **299**, 536 (2003).
[13] J. Full, L. Ganzález, and J. Manz, Chem. Phys. **314**, 143 (2005).
[14] A. Bartelt, A. Lindinger, C. Lupulescu, J. Manz, A. Merli, Š. Vajda, and L. Wöste, Phys. Chem. Chem. Phys. **5**, 3610 (2003).
[15] F. F. Crim, J. Phys. Chem. **100**, 12725 (1996).
[16] I. Bar and S. Rosenwaks, Int. Rev. Phys. Chem. **20**, 711 (2001).
[17] H. F. Davis and Y. T. Lee, J. Chem. Phys. **105**, 8142 (1996).
[18] P. J. Reid, J. Phys. Chem. A **106**, 1473 (2002), and references therein.
[19] K. A. Peterson, J. Chem. Phys. **109**, 8864 (1998).
[20] D. Q. Xie and H. Guo, Chem. Phys. Lett. **307**, 109 (1999).
[21] E. C. Richard and V. Vaida, J. Chem. Phys. **94**, 153 (1991).
[22] T. Baumert, J. L. Herek, and A. H. Zewail, J. Chem. Phys. **99**, 4430 (1993).
[23] M. Blackwell, P. Ludowise, and Y. Chen, J. Chem. Phys. **107**, 283 (1997).
[24] V. Stert, H. H. Ritze, E. T. J. Nibbering, and W. Radloff, Chem. Phys. **272**, 99 (2001).
[25] Z. Sun, N. Lou, and G. Nyman, J. Chem. Phys. **122**, 054316 (2005).
[26] Z. Sun, N. Lou, and G. Nyman, J. Phys. Chem. A **108**, 9226 (2004).
[27] K. J. Yuan, Z. Sun, S. L. Cong, and N. Lou, J. Chem. Phys. **123**, 064316 (2005).
[28] K. J. Yuan, Z. Sun, S. M. Wang, and S. L. Cong, Chem. Phys. Lett. **414**, 180 (2005).
[29] P. Schwendner, F. Seyl, and R. Schinke, Chem. Phys. **217**, 233 (1997).
[30] E. J. Heller, Acc. Chem. Res. **14**, 368 (1981).
[31] Z. Sun, N. Lou, and G. Nyman, Chem. Phys. **308**, 317 (2005).
[32] I. Andrianov, V. Bonačić-Koutecký, M. Hartmann, J. Manz, J. Pittner, and K. Sundermann, Chem. Phys. Lett. **318**, 256 (2000).
[33] G. Marston, I. C. Walker, N. J. Mason, J. M. Gingell, H. Zhao, K. L. Brown, F. Motte-Tollet, J. Delwiche, and M. R. F. Siggel, J. Phys. B **31**, 3387 (1998).
[34] Z. G. Sun, S. L. Cong, N. Q. Lou, and K. L. Han, ChemPhysChem **3**, 976 (2002).
[35] K. A. Peterson and H.-J. Werner, J. Chem. Phys. **96**, 8948 (1992).
[36] Z. Sun, N. Lou, and G. Nyman, Chem. Phys. Lett. **393**, 204 (2004).
[37] A. Paloviita and K. A. Suominen, Phys. Rev. A **55**, 3007 (1997).
[38] K. A. Suominen, B. M. Garraway, and S. Stenholm, Phys. Rev. A **45**, 3060 (1992).